Environmental Science & Technology

pubs.acs.org/est

Article

Unveiling the Sources and Transfer of Mercury in Forest Bird Food Chains Using Techniques of Vivo-Nest Video Recording and Stable Isotopes

Kang Luo, Wei Yuan, Zhiyun Lu, Zichun Xiong, Che-Jen Lin, Xun Wang,* and Xinbin Feng*

Cite This: *Environ. Sci. Technol.* 2024, 58, 6007−6018

Read Online

ACCESS | Metrics & More | Article Recommendations | Supporting Information

ABSTRACT: Knowledge gaps in mercury (Hg) biomagnification in forest birds, especially in the most species-rich tropical and subtropical forests, limit our understanding of the ecological risks of Hg deposition to forest birds. This study aimed to quantify Hg bioaccumulation and transfer in the food chains of forest birds in a subtropical montane forest using a bird diet recorded by video and stable Hg isotope signals of biological and environmental samples. Results show that inorganic mercury (IHg) does not biomagnify along food chains, whereas methylmercury (MeHg) has trophic magnification factors of 7.4−8.1 for the basal resource−invertebrate−bird food chain. The video observations and MeHg mass balance model suggest that Niltava (*Niltava sundara*) nestlings ingest 78% of their MeHg from forest floor invertebrates, while Flycatcher (*Eumyias thalassinus*) nestlings ingest 59% from emergent aquatic invertebrates (which fly onto the canopy) and 40% from canopy invertebrates. The diet of Niltava nestlings contains 40% more MeHg than that of Flycatcher nestlings, resulting in a 60% higher MeHg concentration in their feather. Hg isotopic model shows that atmospheric Hg^0 is the main Hg source in the forest bird food chains and contributes >68% in most organisms. However, three categories of canopy invertebrates receive ∼50% Hg from atmospheric Hg^{2+}. Overall, we highlight the ecological risk of MeHg exposure for understory insectivorous birds caused by atmospheric Hg^0 deposition and methylation on the forest floor.

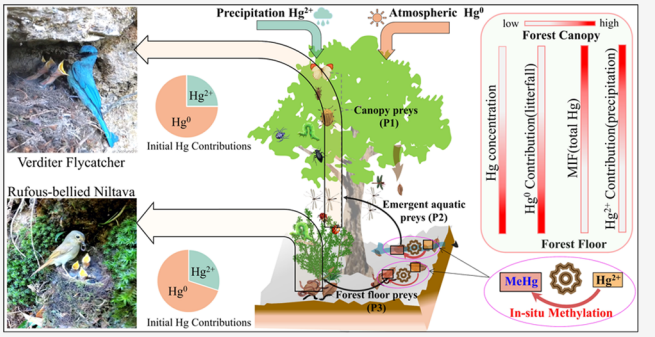

KEYWORDS: *subtropical forest, bird food chain, mercury accumulation, mercury isotopes, vivo-nest video recording*

1. INTRODUCTION

Human activities have significantly increased mercury (Hg) levels in the environment and led to widespread Hg contamination in remote ecosystems,[1−5] where microbiologically induced methylation of inorganic Hg (IHg) produces highly toxic methylmercury (MeHg).[6] The bioaccumulation and biomagnification of MeHg in the food webs pose a threat to the health of wildlife and humans.[6−8] Assessment of Hg levels, sources, biomagnification in wildlife, and the associated impact is crucial for understanding the risk of Hg pollution and for evaluating the effectiveness of control measured outlined in the Minamata Convention on Mercury.[9]

Bacterial transformation of IHg to MeHg in the aquatic system and MeHg exposures through the food chains, including waterbirds and seabirds, have received extensive research attention.[2,6,10] Less understood is the MeHg exposure of bird species in the terrestrial ecosystem.[11−14] Recent studies suggested that forest birds in remote background areas are subject to ecological risks of MeHg exposure.[15−19] Forest birds account for over half of the world's bird species,[20] yet observations on the Hg bioaccumulation in the food chains of forest birds remain relatively scarce, especially in the bird-species-rich tropical/subtropical forests.[11,19,21,22]

Diet and trophic position are key factors in controlling Hg levels in birds.[19,23−25] However, the complexity of forest food chain structures (especially tropical/subtropical forests) poses a challenge to determine the trophic niche (i.e., diet and trophic level) of forest birds.[26] The preys of forest birds mainly consist of invertebrates, such as insects, which are diverse in species, small in size, and thus difficult to categorize.[26] Earlier studies have utilized nutrient isotopic tracers (e.g., $\delta^{13}C$ and $\delta^{15}N$) to identify the diet compositions and trophic positions of birds.[19,23−25] However, $\delta^{13}C$ and $\delta^{15}N$ signals do not directly indicate the sources of Hg in the food chains or the specific Hg biogeochemical processes along the forest vertical

Received: December 26, 2023
Revised: March 5, 2024
Accepted: March 11, 2024
Published: March 21, 2024

structures (e.g., Hg methylation in the forest floor and Hg accumulation in the canopy).[27−29] Recently, the advancement of high-resolution video recording provides a direct identification and quantification of the diet for forest bird nestlings.[22,30,31] Supplemented with a stable Hg isotope signal of biological samples, it presents a new opportunity to understand the exposure risks of forest birds to MeHg.[32]

The Hg isotopic fractionations exhibit three unique dimensional characteristics: the mass-dependent fractionation (MDF, expressed as δ^{202}Hg), odd mass-independent fractionation (odd-MIF, Δ^{199}Hg, and Δ^{201}Hg), and even mass-independent fractionation (even-MIF, Δ^{200}Hg, and Δ^{204}Hg).[32,33] Hg-MDF is generated by most kinetics processes and equilibrium exchange of Hg.[32] However, the Hg odd- and even-MIF are basically absent during Hg bioaccumulation in food chains,[34−36] thus, as a vivo tracer to identify the sources and processes of Hg along the bird food chains.[37,38] For example, MIF signals of the MeHg in resident songbird feathers have been identified as an efficient tool to reconstruct MeHg sources in a Hg mining region.[39]

Overall, bird foraging microhabitat niche and diet compositions likely determine Hg source and exposure risk given differences in Hg biogeochemical processes among forest vertical structures (i.e., forest floor to canopy).[3,40,41] Thus, we hypothesized that the Hg exposure risk for birds hunting on the understory layer would be significantly different from that for birds hunting on the canopy. Herein, this study aimed to examine the source contributions and bioaccumulations of Hg in the food chains of two sympatric forest insectivorous passerines, the Rufous-bellied Niltava (*Niltava sundara*, hunting on the understory layer primarily) and the Verditer Flycatcher (*Eumyias thalassinus*, hunting in the upper canopy layer), in a primary subtropical forest of Mt. Ailao. We used video observations and an isotopic tool to determine Hg exposure in forest birds and to quantify the contribution of Hg sources in their food chains. Finally, we discussed the implications of the relations of bird foraging niches to Hg exposure risk in forests.

2. METHODS

2.1. Site Description. Our study site is located within the experimental area of the Ailaoshan Station for Subtropical Forest Ecosystem Research Studies (24°32′N, 101°01′E, 2500 m elevation), Mt. Ailao, Yunnan province, SW China. Detailed information on Mt. Ailao has been described in our previous studies.[42−44] Briefly, Mt. Ailao has a subtropical monsoon climate with an average annual temperature of 11 °C and an average annual rainfall of 1682 mm. The vegetation is dominated by subtropical forest tree species such as Fagaceae, Theaceae, Lauraceae, and Magnoliaceae.[4545] Mt. Ailao is a National Nature Reserve with rich biodiversity including over 500 bird species and has been designated as an Important Bird Area (IBA) by Birdlife International.[46]

2.2. Prey Composition of Nestling. We searched bird nests along the transects and rechecked them every 1−4 days to acquire breeding information and perform sampling of bird feathers. We selected the nests with nestlings of known age to record provisioning events and recognize prey composition.[22,30] Additionally, we observed the foraging microhabitat of adult birds (i.e., Niltava and Flycatcher, the dominant species in Mt. Ailao with potentially different foraging microhabitat niches) to ensure the subsequent prey sampling. Additional details on bird-nest searching, rechecking, video recording, and adult foraging behavior observation can be found in Section S1, Supporting Information (SI).

2.3. Sampling. *2.3.1. Sampling for Basal Resources.* Based on the forest vertical structure, we selected three types of microhabitats, namely, forest floor layer (i.e., the ground surface layer containing humus and litterfall), water body layer (i.e., small creeks and ponds), and canopy layer (referring to the aboveground vertical structures of forest stands such as leaves, branches, and stems). We collected five types of basal resources, including litterfall, humus (highly decomposed litterfall), litterfall-submerged (litterfall that was submerged in a water body), detritus-submerged (highly decomposed detritus that was submerged in a water body), and fresh leaves.

2.3.2. Sampling for Invertebrates. Based on the field observations of adult birds' foraging events and video recordings of prey provisioning to nestlings, we collected prey samples from the corresponding feeding microhabitats. We employed sweep nets, beating trays, sieves, and light traps to capture invertebrates and recorded their weight. The invertebrates were categorized according to their original habitat layer, including canopy invertebrates, forest floor invertebrates, and emergent aquatic invertebrates from the water body.

2.3.3. Sampling for Nestlings. To ensure consistency in our sampling, we selected target species (i.e., Niltava and Flycatcher) with known ages of nestlings and sampled three nests of each species. More detailed information on sampling procedures and sample preparations can be found in Section S2, SI.

2.4. Chemical Analysis. *2.4.1. Hg Determination.* THg concentrations of the basal resources (i.e., litterfall, humus, litterfall-submerged, detritus-submerged, and fresh leaves) were measured by using a DMA-80 Hg analyzer.[3,42,47−50] We determined Hg concentrations of one certified reference material (CRM) and one parallel sample in every four samples. The CRM of GBW07404a (GSS-4a) and NIST 1515 was utilized for quality assurance/quality control (QA/QC) with a recovery of 98.1 ± 3.7% (n = 6). The bias between the parallel samples was 1.8 ± 1.2% (n = 3). MeHg concentrations of the basal resources were measured using gas chromatography coupled with a cold-vapor atomic fluorescence spectrometer (GC-CVAFS, Brooks Rand III) in accordance with the USEPA Method 1630[19,22,51,52] (more details in Section S3). The ERM CC580 (n = 4) and TORT-3 (n = 2) were utilized for QA/QC with a recovery of 96.7 ± 6.9% (n = 6). The bias between the parallel samples was 5.3 ± 2.2% (n = 3).

A modified method was applied to determine THg and MeHg simultaneously in invertebrates and feathers.[51,53,54] THg was determined using cold-vapor atomic absorption spectrometry (CVAFS, Brooks Rand Model III), following the USEPA method 1630E.[51] MeHg was determined using the GC-CVAFS method (more details in Section S3). For THg measurements, we used the GBW07601a (n = 5) and TORT-3 (n = 7) for QA/QC with a recovery of 98.2 ± 9.1%. The bias of the parallel samples was 3.9 ± 2.6% (n = 9). For MeHg measurements, we used the TORT-3 (n = 7) for QA/QC with a recovery of 88.5 ± 5.7%. The bias of the parallel samples was 5.3 ± 1.7% (n = 8).

2.4.2. Stable Isotope Analysis. δ^{13}C and δ^{15}N isotope ratios were measured by using a gas mass spectrometer (MAT 253, Thermo Scientific, Germany). The stable isotope ratios are reported in per mill (δ) notation as follows

https://doi.org/10.1021/acs.est.3c10972
Environ. Sci. Technol. 2024, 58, 6007−6018

$$\delta X = \left(\frac{R_{sample}}{R_{std}} - 1\right) \times 1000 \quad (1)$$

where X represents ^{15}N and ^{13}C. R_{sample} and R_{std} represent the abundance ratios of $^{15}N/^{14}N$ and $^{13}C/^{12}C$ in samples and standardized materials, respectively. The quality control of $\delta^{13}C$ and $\delta^{15}N$ isotope measurements was performed using certified recovery materials C-3 ($\delta^{13}C$ = −24.750‰) and N-1 ($\delta^{15}N$ = 0.417‰) of the International Atomic Energy Agency. Variations in both $\delta^{13}C$ and $\delta^{15}N$ in CRMs were <0.1‰, which confirms the accuracy of isotopic measurements.

For Hg isotopic compositions, litterfall, humus, litterfall-submerged, and detritus-submerged samples were digested with aqua regia (HNO_3/HCl = 3:1). Other samples (e.g., fresh leaves, invertebrates, and feathers) were digested with ultrapure HNO_3.[51,55] More details can be found in Section S3 of the SI. THg was determined using the CVAFS method with the recovery of CRMs (GSS-4, BCR-482, and TORT-3) being 94.3 ± 8.8% (n = 6).

Prior to Hg isotope analysis, the digestion solution was adjusted to ∼1 ng mL^{-1} and 10% acidity.[55,56] The Hg isotopic compositions were determined by a multicollector inductively coupled plasma mass spectrometer (MC-ICP-MS, Nu-Plasma II, Thermo Scientific). According to Bergquist and Blum,[57] the Hg-MDF is reported as

$$\delta^{202}Hg\ (‰) = 1000 \times [(^{202}Hg/^{198}Hg_{sample}) / (^{202}Hg/^{198}Hg_{NIST\text{-}3133}) - 1] \quad (2)$$

where $(^{202}Hg/^{198}Hg_{NIST\text{-}3133})$ represents the isotopic ratio in the standard sample (NIST-3133). The MIF is calculated as

$$\Delta^{199}Hg(‰) = \delta^{199}Hg - 0.2520 \times \delta^{202}Hg \quad (3)$$

$$\Delta^{200}Hg(‰) = \delta^{200}Hg - 0.5024 \times \delta^{202}Hg \quad (4)$$

$$\Delta^{201}Hg(‰) = \delta^{201}Hg - 0.7520 \times \delta^{202}Hg \quad (5)$$

To evaluate the potential isotopic composition bias during preconcentration, we determined the Hg isotopic compositions of BCR-482 (vegetation CRM), GSS-4 (soil CRM), and TORT-3 (animal CRM) in every 10 samples. The Hg isotopic signatures of BCR-482 were measured as $\delta^{202}Hg$ = −1.36 ± 0.09‰, $\Delta^{199}Hg$ = −0.61 ± 0.01‰, $\Delta^{200}Hg$ = −0.06 ± 0.01‰, and $\Delta^{201}Hg$ = −0.61 ± 0.05‰ (mean ± 2SD, standard deviation, n = 3); for GSS-4 as $\delta^{202}Hg$ = −1.68 ± 0.17‰, $\Delta^{199}Hg$ = −0.43 ± 0.06‰, $\Delta^{200}Hg$ = −0.04 ± 0.03‰, and $\Delta^{201}Hg$ = −0.40 ± 0.07‰ (n = 4); and for TORT-3 as $\delta^{202}Hg$ = 0.10 ± 0.10‰, $\Delta^{199}Hg$ = 0.62 ± 0.08‰, $\Delta^{200}Hg$ = 0.06 ± 0.07‰, and $\Delta^{201}Hg$ = 0.51 ± 0.07‰ (n = 10). The NIST-8610 was also analyzed for every 10 samples during the Hg isotope measurements, with isotopic signatures of $\delta^{202}Hg$ = −0.51 ± 0.11‰, $\Delta^{199}Hg$ = −0.01 ± 0.05‰, $\Delta^{200}Hg$ = 0.00 ± 0.07‰, and $\Delta^{201}Hg$ = −0.03 ± 0.06‰ (n = 21). The measured Hg isotopic signatures of CRMs were consistent with the recommended values.[35,58,59]

2.5. Data Analysis. Inorganic mercury (IHg) concentrations in the samples were calculated as the concentration difference between THg and MeHg. All concentrations are reported in dry weight. The trophic level (TL) was calculated as[60]

$$TL = (\delta^{15}N_{predator} - \delta^{15}N_{basal\text{-}resources})/3.4‰ + 1 \quad (6)$$

where $\delta^{15}N_{predator}$ represents the $\delta^{15}N$ values of biota and $\delta^{15}N_{basal\text{-}resources}$ represents the $\delta^{15}N$ value in the primary producer (i.e., fresh leaves in our study). The trophic magnification slope (TMS) was calculated as follows[61]

$$\log_{10}[XHg] = TMS \times \delta^{15}N + a \quad (7)$$

The biota-soil accumulation factor (BSAF)[62] was utilized to quantify the Hg biomagnification from basal resources to the invertebrates, and it was calculated as follows[62,63]

$$BSAF = XHg_{invertebrates}/XHg_{basal} \quad (8)$$

We used the apparent biomagnification factor (ABMF), which is defined as the ratios of Hg concentrations among bird−prey pairs according to previous research.[63−65] The calculation of ABMF is as follows

$$ABMF_{XHg} = XHg_{predator}/XHg_{prey} \quad (9)$$

where XHg represents the MeHg or IHg concentrations in bird and prey (invertebrates) and basal resources, respectively. The TMS > 0, BSAF or ABMF > 1 indicates the biomagnification of Hg in the food chain. It is noted that the ABMF only reflects the potential MeHg biomagnification due to the bird obtaining food from a variety of sources.

Trophic magnification factor (TMF), which represents the average biomagnification per TL through the entire food web, was calculated as follows[23]

$$Log_{10}[XHg] = B \times TL + A \quad (10)$$

$$TMF = 10^{B} \quad (11)$$

Hg mass intake by nestlings is estimated by

$$MassXHg_{bird(intake)} = \frac{\sum_{i=1}^{n}(f_i \times T \times m_i \times XHg_i)}{F_i \times N} \quad (12)$$

where XHg represents MeHg or IHg. $MassXHg_{bird(intake)}$ is the Hg mass intake by each nestling (including MeHg and IHg). f_i is the proportion of invertebrates i in the total provisioning trips, F_i is the total proportion of measured prey to the total provisioning trips, T is the total numbers of provisioning trips during a 15 day nestling period, m_i is the average dry weight of invertebrates i, XHg_i is the Hg concentration of invertebrates i (including MeHg and IHg), and N is the average nestling number of the video-recorded nests (for Niltava is 3.2 and 4.2 for Flycatcher). In addition, combining the Hg mass intake by nestlings and Hg isotope signatures of prey, we also predicted the Hg isotopes of the nestlings (details in Section 4, SI).

Three source endmembers have been identified for the initial Hg sources in forest ecosystems, including atmospheric Hg^{2+} deposition, atmospheric Hg^0 deposition, and geogenic sources.[4,50,66−68] The organisms in the forest food chain do not feed on rocks. The Hg concentrations of basal resources (excluding the fresh leaves) are more than 1 order of magnitude higher than those of rocks (e.g., 161.2 ± 78.7 versus 4.2 ± 1.4 ng g^{-1}).[44] Hence, the contribution of geogenic Hg to forest bird food chains can be neglected. Given the absence of even-MIF ($\Delta^{200}Hg$) processes in forests,[69,70] we estimated contributions of atmospheric Hg^{2+} and atmospheric Hg^0 to the forest bird food chains using the Hg even-MIF mixing model

$$f_1 + f_2 = 1 \quad (13)$$

https://doi.org/10.1021/acs.est.3c10972
Environ. Sci. Technol. 2024, 58, 6007−6018

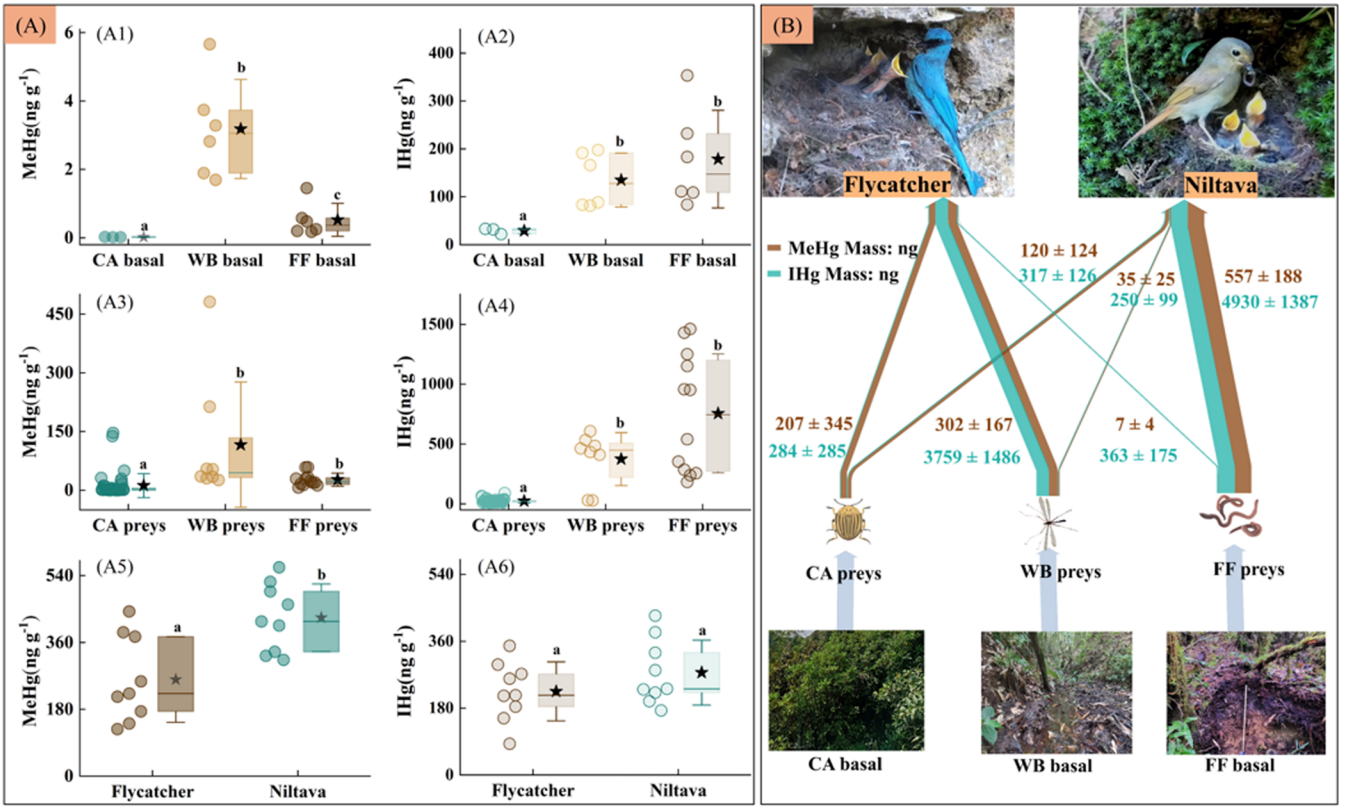

Figure 1. Changes of methylmercury (MeHg) and inorganic mercury (IHg) (on dry weight basis, ng g^{-1}) in the organisms along the forest bird food chains (A). The arrows between birds and prey items indicate the transfer of Hg mass from invertebrates to bird nestlings (B). Boxplot elements in panels (A–F) show the median (midline), mean (star), the interquartile range of 25 and 75% percentile (box boundaries), data points, and standard deviation. The letter in (A1)–(A6) denotes the statistical difference at the 95% confidence level. CA is short for canopy, WB for water body, and FF for forest floor.

$$\Delta^{200}Hg_1 \times f_1 + \Delta^{200}Hg_2 \times f_2 = \Delta^{200}Hg_{organisms} \quad (14)$$

where f_1 is the atmospheric Hg^{2+} input contribution and f_2 is the atmospheric Hg^0 input contribution. $\Delta^{200}Hg_1$ is the signature of atmospheric Hg^{2+} inputs and obtained from our previous results at Mt. Ailao (0.23 ± 0.04‰, 1SD).[71] $\Delta^{200}Hg_2$ is the signature of atmospheric Hg^0 inputs (represented by the foliage, −0.07 ± 0.04‰, 1SD). We used Monte Carlo simulations to quantify uncertainties of the model results.[4,50] These uncertainties are quantified by generating one million groups of MIF signatures randomly ranging from mean − SD to mean + SD to solve the Hg isotope mixing model. (The R script can be found in Section S5, SI.)

Statistical analyses and linear fits were performed using Origin Pro 2020 (Learning edition, Origin Lab). One-way analysis of variance (ANOVA) was used for the significance analysis when the data were normally distributed. Otherwise, the Kruskal–Wallis test was used. The Pearson correlation analysis was used to evaluate the correlation between the variables. The significance levels were at $P \leq 0.05$.

3. RESULTS

3.1. Analysis of Diet Composition of the Nestlings from Video Recordings. We obtained high-resolution recordings of 70 h from six Niltava nests with 1226 food trips and 80 h from seven Flycatcher nests with 1550 food trips. We identified 1126 of 1226 provisioning trips (91.8%) in Niltava recordings and 1324 of 1550 provisioning trips in Flycatcher recordings (85.4%). More details can be found in Table S1. The prey mass was measured in 18 categories of prey for Niltava (70.7% of total provisioning visits) and 15 categories of prey for Flycatcher (75.2%). The dry weight of prey provided by adult birds to each nestling was estimated based on visit frequency, nestling days, and prey dry weights (Table S2). For the Flycatcher, the biggest dry mass estimation (62.9%) came from canopy invertebrates (13.6 ± 12.4 g), followed by emergent aquatic invertebrates (7.7 ± 1.9 g, 35.5%), and the lowest from forest floor invertebrates (0.3 ± 0.1 g, 1.6%). The Niltava had the largest dry mass estimation (55.1%) from canopy invertebrates (16.1 ± 4.9 g), followed by forest floor invertebrates (12.6 ± 1.0 g, 43.1%) and emergent aquatic invertebrates (0.6 ± 0.1 g, 1.8%). More information on bird ecological surveys is in Section S1, SI.

3.2. Hg Concentrations in the Forest Food Chains. Figure 1A shows variations of MeHg and IHg in the food chain components (Table S3). For the basal resources, the water body (i.e., detritus-submerged) had the highest MeHg concentrations (3.2 ± 1.5 ng g^{-1}, $n = 6$), followed by the forest floor (i.e., litterfall and humus) with the 0.5 ± 0.5 ng g^{-1} ($n = 6$), and then the canopy (i.e., fresh leaves) with a value of 0.02 ± 0.01 ng g^{-1} ($n = 3$). The IHg concentrations in canopy fresh leaves (28.9 ± 6.1 ng g^{-1}) were significantly lower than those of forest floor (IHg = 178.8 ± 101.8 ng g^{-1}) and water body (IHg = 134.8 ± 54.2 ng g^{-1}) (all $P < 0.05$), but there was no significant difference between IHg concentrations in basal resources of forest floor and water body ($P > 0.05$).

Invertebrates showed a similar pattern to basal resources. The canopy invertebrates (MeHg = 5.7 ± 10.3 ng g^{-1}, IHg =

https://doi.org/10.1021/acs.est.3c10972
Environ. Sci. Technol. 2024, 58, 6007−6018

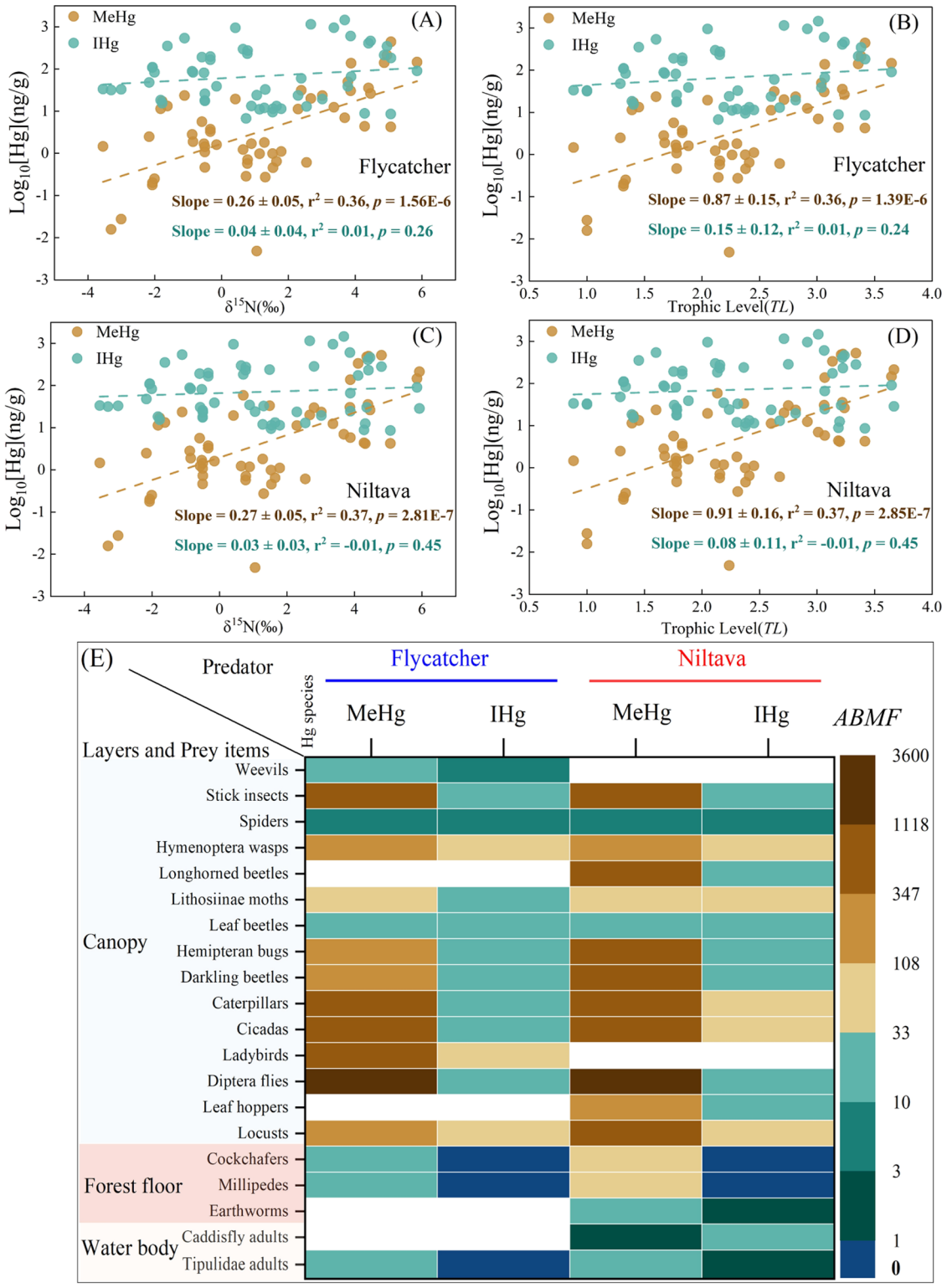

Figure 2. Linear regressions between $\log_{10}$[MeHg] or [IHg] and δ^{15}N and trophic levels (TLs) for Flycatcher nestlings (A, B) and Niltava nestlings (C, D); heatmap of the apparent biomagnification factors (ABMFs) for bird−prey pairs (E). Blank cells in panel (E) indicate that no instances of predation between the bird−prey pairs were found. The heatmap displayed the computation of the mean values for each species/category, and Table S5 includes the ABMFs based on min, max, and median.

21.3 ± 11.5 ng g^{-1}, n = 42; two spiders were excluded due to outlier values) had the lowest concentrations compared to those of the forest floor invertebrates (MeHg = 24.2 ± 15.4 ng g^{-1}, IHg = 680.5 ± 462.1 ng g^{-1}, n = 9) and the emergent aquatic invertebrates (MeHg = 116.2 ± 159.8 ng g^{-1}, IHg = 373.9 ± 221.1 ng g^{-1}, n = 8) (all $P < 0.05$). There was no significant difference in the MeHg and IHg concentrations between the forest floor and emergent aquatic invertebrates (all $P > 0.05$). The IHg concentration was comparable in the feather of Niltava and Flycatchers nestlings (224.9 ± 79.6

https://doi.org/10.1021/acs.est.3c10972
Environ. Sci. Technol. 2024, 58, 6007−6018

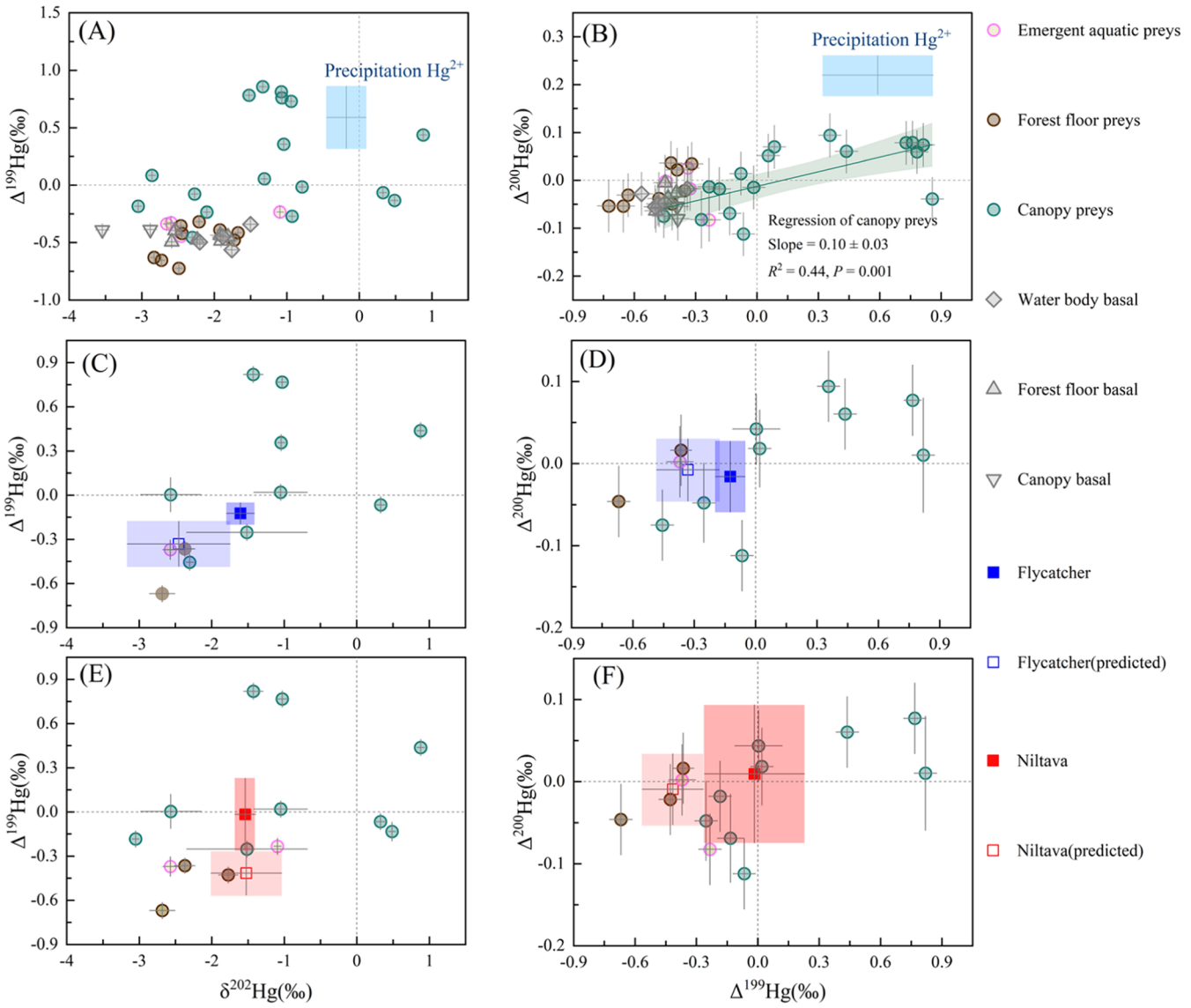

Figure 3. Hg isotopic signatures of basal resources and invertebrates (prey items) in panels (A) and (B). The Hg isotopic signatures of precipitation were obtained from an earlier study at Mt. Ailao.[71] The Hg isotopic fingerprints of bird nestlings and their prey items ((C) and (D) for Flycatcher, (E) and (F) for Niltava). The filled boxes represent the measured Hg isotopes of the birds, while open boxes refer to the predicted values (and SD). The error bar represents ±1 standard deviation (1σ). The shaded boxes in panels (A) and (B) indicate the SD range of the isotopes of precipitation Hg^{2+}, and panels (C)−(F) indicate the SD range of the Hg isotopes for the predicted and measured values of the nestlings. Panels (A)−(F) share the same legend items.

versus 275.6 ± 87.5 ng g^{-1}, $P > 0.05$), but a significant difference was in MeHg (426.5 ± 91.1 versus 260.1 ± 115.0 ng g^{-1}, $P < 0.05$).

3.3. Hg Transfer from Invertebrates to Birds. The arrows in Figure 1B show the transfer of the Hg mass from invertebrates to birds. Each Niltava nestling took up 712 ± 227 ng MeHg during 15 days of observations, with 78% of total MeHg from forest floor invertebrates (557 ± 188 ng). Each Flycatcher nestling took up 516 ± 383 ng MeHg with 59% from emergent aquatic invertebrates (302 ± 167 ng) and 40% from canopy invertebrates (207 ± 345 ng). For IHg, each Niltava nestling took up 5497 ± 1396 ng with 90% of IHg from the forest floor invertebrates (4930 ± 1387 ng). The Flycatcher took up 4406 ± 1523 ng IHg with 86% from the emergent aquatic invertebrates (3759 ± 1486 ng).

3.4. Hg Bioaccumulation in Forest Food Chains. We observed a significant increase of $\delta^{13}C$ and $\delta^{15}N$ values from basal resources of the canopy (i.e., fresh leaves) to those of the forest floor (i.e., litterfall and humus) and the water body (i.e., litterfall-submerged and detritus-submerged) ($R^2 = 0.69$, $P < 0.01$; Figure S1). The trophic levels (TLs) of the organisms from the forest bird food chains ranged from 0.9 to 3.7 (Tables S4 and S7).

Significant biomagnification of MeHg occurred in the two food chains but not for the IHg. For the flycatcher's food chain, TMS_{MeHg} was 0.26 ± 0.05 and TMF_{MeHg} was 7.4 ± 1.4. For Niltava, the food chain, TMS_{MeHg} was 0.27 ± 0.05 and TMF_{MeHg} was 8.1 ± 1.5. The values of $\log_{10}$ IHg to $\delta^{15}N$ showed an insignificant correlation to the trophic levels (TLs) in two food chains (Figures 2A−D and S3). We calculated the apparent biomagnification factor (ABMF) based on the mean, minimum, maximum, and median MeHg and IHg concentrations of each category. Ninety-nine percent of $ABMF_{MeHg}$ and 81% of $ABMF_{IHg}$ were greater than 1 (Table S5). The

https://doi.org/10.1021/acs.est.3c10972
Environ. Sci. Technol. 2024, 58, 6007−6018

$ABMF_{MeHg}$ exhibited higher values than the $ABMF_{IHg}$, and the highest ABMFs were found in bird−canopy prey pairs (e.g., $ABMF_{MeHg}$ up to 26 304 and $ABMF_{IHg}$ up to 39 for Flycatcher), followed by bird−forest floor prey pairs (e.g., $ABMF_{MeHg}$ up to 19 and $ABMF_{IHg}$ up to 0.3 for Flycatcher), and then bird−water body prey pairs (e.g., $ABMF_{MeHg}$ up to 8 and $ABMF_{IHg}$ up to 0.6 for Flycatcher) in Figure 2E.

3.5. Hg Isotopic Signatures in Forest Food Chains. Figure 3 shows the Hg isotopic compositions (Tables S6 and S8). The fresh leaves of the canopy exhibited average values of $\delta^{202}Hg = -3.21 \pm 0.47‰$, $\Delta^{199}Hg = -0.39 \pm 0.04‰$, and $\Delta^{200}Hg = -0.07 \pm 0.04‰$ ($n = 3$). The litterfall and humus of the forest floor exhibited average values of $\delta^{202}Hg = -2.17 \pm 0.34‰$, $\Delta^{199}Hg = -0.46 \pm 0.04‰$, and $\Delta^{200}Hg = -0.04 \pm 0.04‰$ ($n = 6$). The litterfall-submerged and detritus-submerged in water had average values of $\delta^{202}Hg = -1.8 \pm 0.26‰$, $\Delta^{199}Hg = -0.49 \pm 0.10‰$, and $\Delta^{200}Hg = -0.02 \pm 0.04‰$ ($n = 5$).

The forest floor invertebrates showed average values of $\delta^{202}Hg = -2.28 \pm 0.42‰$, $\Delta^{199}Hg = -0.49 \pm 0.15‰$, and $\Delta^{200}Hg = -0.02 \pm 0.04‰$ ($n = 9$), comparable to the values of their food sources (all $P > 0.05$). The emergent aquatic invertebrates showed average values of $\delta^{202}Hg = -2.20 \pm 0.74‰$, $\Delta^{199}Hg = -0.34 \pm 0.09‰$, and $\Delta^{200}Hg = -0.02 \pm 0.05‰$ ($n = 4$). The $\Delta^{199}Hg$ of the emergent aquatic insects was $0.15 \pm 0.13‰$ higher than the values of their food sources ($P < 0.05$). The canopy invertebrates showed a large range of Hg isotopes, with an average $\delta^{202}Hg$ of $-1.23 \pm 1.10‰$, $\Delta^{199}Hg$ of $0.20 \pm 0.44‰$, and $\Delta^{200}Hg$ of $0.01 \pm 0.07‰$ ($n = 17$). Both their $\delta^{202}Hg$ and $\Delta^{199}Hg$ were higher than the values of their food sources ($P < 0.05$, by the Kruskal−Wallis test). The canopy invertebrates also showed significantly higher $\delta^{202}Hg$ and $\Delta^{199}Hg$ values than the forest floor invertebrates and the emergent aquatic invertebrates (all $P < 0.05$). A significant positive correlation existed between $\Delta^{199}Hg$ and $\Delta^{200}Hg$ of the canopy invertebrates and leaves (Figures 3B and S4).

The Hg isotopic signatures of nestling feathers of two bird species were within the range of their preys. No significant differences between the Hg isotopic compositions of the two bird species were found (for Flycatcher: $\delta^{202}Hg = -1.60 \pm 0.19‰$, $\Delta^{199}Hg = -0.12 \pm 0.07‰$, $\Delta^{200}Hg = -0.02 \pm 0.04‰$; and for Niltava: $\delta^{202}Hg = -1.54 \pm 0.14‰$, $\Delta^{199}Hg = -0.02 \pm 0.24‰$, $\Delta^{200}Hg = 0.01 \pm 0.08‰$).

4. DISCUSSION

4.1. MeHg Biomagnification from Basal Resources to Invertebrates. The MeHg levels of basal resources follow the descending order of water body > forest floor > the canopy. The higher MeHg levels in the water body and forest floor basal resources are caused by the higher IHg concentrations and anoxic conditions favoring the microbial conversion of IHg to MeHg.[2,6,10] The positive shifts in $\delta^{13}C$ and $\delta^{15}N$ during the litterfall decomposition process ($R^2 = 0.69$, $P < 0.01$; Figure S1) also indicate the degradation of litter by bacteria and/or fungi.[54] The higher shifts of $\delta^{13}C$ than $\delta^{15}N$ can be explained by the much faster C mineralization than N during the litter decomposition processes.[72,73]

We observed that the biota-soil accumulation factor of MeHg ($BSAF_{MeHg}$) for the invertebrate−basal pairs was highest in the canopy, followed by the forest floor and then the water body (Table S6). The highest $BSAF_{MeHg}$ of invertebrate−basal pairs in the canopy is due to the very low MeHg concentration in fresh leaves, thus magnifying the value of $BSAF_{MeHg}$.[61,74] The forest floor invertebrates and the emergent aquatic invertebrates have a MeHg concentration 5−20 times higher than the value of the canopy invertebrates, respectively (Figure 1A). The elevated MeHg concentrations in forest floor invertebrates and emergent aquatic invertebrates are contributed by two factors. One is the much higher MeHg levels in basal resources of the water body and the forest floor. The other is a longer food chain. The trophic levels depicted by $\delta^{15}N$ suggest that the canopy invertebrates have the shorter food chain lengths than the emergent aquatic invertebrates (2.3 ± 0.7 versus 3.3 ± 0.2, $P < 0.05$; Figure S2). MeHg concentrations in emergent aquatic invertebrates span a large range (Figure 1B), indicating the complexity of the food chains. The earlier study showed that the detritus was initially transformed into bacterial and fungal biomass, then consumed by small predators (e.g., protists), and finally consumed by invertebrates.[75] Some invertebrates also directly consumed detritus and litters.[54,61] The longer food chain could lead to greater MeHg biomagnification in invertebrates.

4.2. Foraging Microhabitat Niche Influencing the Hg Biomagnification. The forest located at Mt. Ailao, SW China, has been identified as a distinct atmospheric Hg sink with an annual deposition of 50−80 $\mu g\ m^{-2}\ year^{-1}$.[72,76] Thus, we speculated that forest birds at Mt. Ailao could face high risks of MeHg exposure. The nestling feather MeHg levels (426.5 ± 91.1 for Niltava and 260.1 ± 115.0 ng g^{-1} for Flycatchers) in our study are significantly higher than previous observations on typical insectivorous Tit nestlings from the remote pine forest (*Parus major*, 79.1 ± 28.0 ng g^{-1})[30,51] and urban green parks (*Parus monticolus*, 115 ± 31 ng g^{-1})[52] in subtropical regions. Additionally, MeHg levels in our study are comparable to those of Phoebe nestlings (*Sayornis phoebe*, 420 ± 180 ng g^{-1}) in a temperate forest highly impacted by the agriculture load inputs.[77] These comparisons confirm our hypothesis of a high Hg exposure risk to forest birds at Mt. Ailao.

Insectivorous songbirds are recognized to be highly vulnerable to the adverse effects of mercury (Hg) exposure.[19,23,78] However, few studies discussed the impact of foraging microhabitat niches on the risks of Hg exposure among sympatric insectivorous songbirds. The sampling in this work was conducted in the same habitats within a narrow geographic region (the furthest sampling nest was less than 4 km away) using consistent tissues (feathers of 15 day old nestlings). These allowed examination of the effect of the species-specific foraging microhabitat niche on Hg exposure.

In both food chains, MeHg was biomagnified significantly, with little biomagnification for IHg. The feather of Niltava nestling had significantly higher MeHg levels than the feather of Flycatcher nestling (426.49 ± 91.16 versus 260.07 ± 115.05 ng g^{-1}, $P < 0.05$) due to the stronger MeHg biomagnification of Niltava compared to that of Flycatcher (8.1 ± 1.5 versus 7.4 ± 1.4 in per trophic level).

The difference in the foraging microhabitat niche is the main cause for the elevated MeHg level in the feather of Niltava nestling. Niltava hunts in the understory layer primarily (e.g., forest floor and lower canopy), while Flycatcher generally hunts in the upper canopy layer (Section S1). Flycatcher nestling food is primarily sourced from canopy invertebrates and emergent aquatic invertebrates. In contrast, Niltava nestling food is mainly sourced from lower canopy invertebrates and forest floor invertebrates (Table S2). The

https://doi.org/10.1021/acs.est.3c10972
Environ. Sci. Technol. 2024, 58, 6007−6018

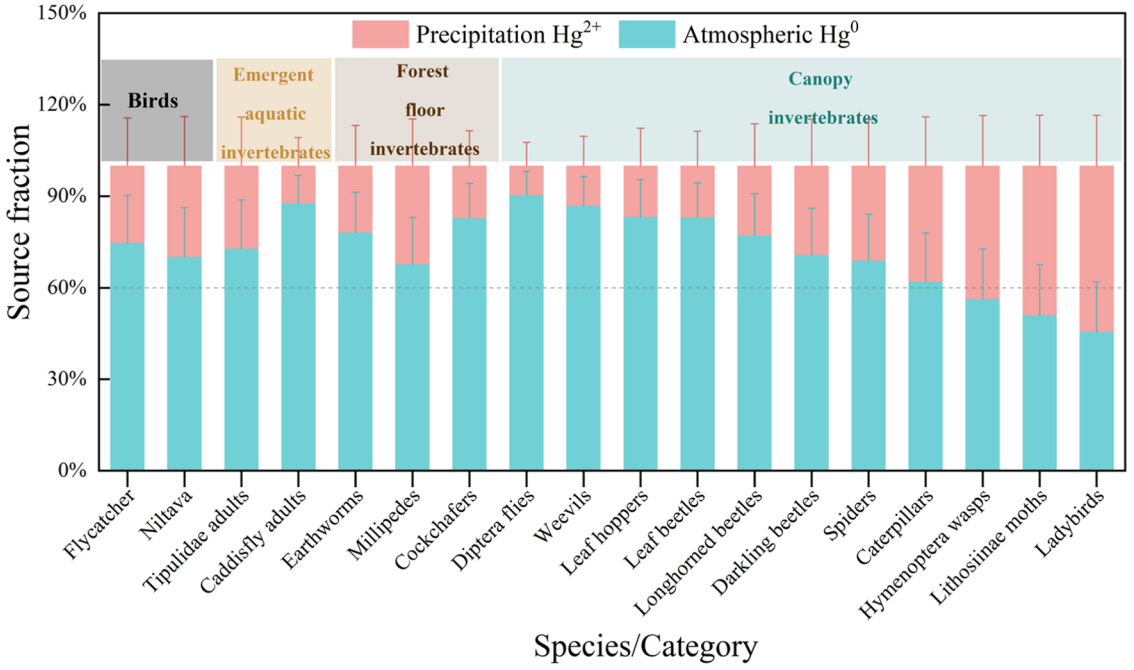

Figure 4. Results of Hg isotopic mixing model showing source contribution of atmospheric Hg^0 and precipitation Hg^{2+} to the organisms along the forest bird food chains.

MeHg levels in the forest floor invertebrates much higher than those in the canopy invertebrates transfer more MeHg from invertebrates to Niltava nestlings (Figure 1).

A distinct MeHg mass transfer from emergent aquatic invertebrates to Flycatcher nestlings was also identified. This is because the emergent aquatic invertebrates (e.g., *Tipulidae* spp.) bloomed during the observation period and these invertebrates flew to the upper canopy and were preyed on by the Flycatcher. This study illustrates that MeHg can be transferred from aquatic to terrestrial ecosystems. Earlier studies also showed that the emergent invertebrates were the primary cause of the elevated MeHg levels observed in songbirds nearby the aquatic ecosystems.[39,77,78]

4.3. Hg Isotopic Signals in Forest Bird Food Chains. We observed similar δ^{202}Hg values in both forest floor invertebrates and their basal resources as well as in the emergent aquatic invertebrates and their basal resources. This indicates that the insignificant MDF occurs during the transfer of Hg at low trophic levels.[34,36,38] It is noted that the mechanisms of δ^{202}Hg shift in the trophic level transfer or internal metabolism in invertebrates are still poorly understood.[29,36]

The insignificant difference in Δ^{199}Hg between the forest floor invertebrates and their basal resources also suggests that the small odd-MIF occurs during the Hg trophic transfer. The Δ^{199}Hg values in the emergent aquatic invertebrates were similar to those in forest floor invertebrates, rather than sharing the positive value found in the rainfall (atmospheric Hg^{2+}, 0.48 ± 0.02‰).[71] The original food and nutrient resources for emergent aquatic invertebrates are from detritus-submerged due to little plankton being found in these water bodies. Another possible cause for the negative Δ^{199}Hg value in the emergent aquatic invertebrate is that the input of upland forest runoff water is likely associated with the negative Δ^{199}Hg signals due to the forest organic soil Hg dissolution.[79,80] Given that Δ^{199}Hg in emergent aquatic invertebrates is 0.15 ± 0.13‰ higher than those in detritus-submerged, a fraction of atmospheric Hg^{2+} deposition was also possibly incorporated into the food resources of emergent aquatic invertebrates.

The δ^{202}Hg and Δ^{199}Hg values in the canopy invertebrate samples (δ^{202}Hg = −1.23 ± 1.10‰, Δ^{199}Hg = 0.20 ± 0.44‰, n = 17) were much more positive than those of fresh leaves, as well as of invertebrates from the forest floor and the water body (all $P < 0.05$). A portion of invertebrate samples exhibited positive Δ^{200}Hg values (up to 0.09 ± 0.07‰, 2SD). A significant positive correlation was found between Δ^{199}Hg and Δ^{200}Hg in canopy invertebrates and leaves (R^2 = 0.44, P = 0.001; Figures 3B and S4). These Hg isotopic shifts of canopy invertebrates cannot be explained by microbial/photodegradation of MeHg (or reduction of Hg^{2+})[27,38] or internal metabolism of Hg by invertebrates,[29,36] since these processes do not induce an even-MIF. Given the positive values of Δ^{199}Hg and the positive Δ^{200}Hg signals in atmospheric Hg^{2+}[81] and the elevated precipitation Hg^{2+} deposition flux (29.7 μg m^{-2} $year^{-1}$) at Mt. Ailao,[82] we speculated that a fraction of atmospheric Hg^{2+} was incorporated into canopy invertebrates, causing the positive Δ^{200}Hg and Δ^{199}Hg values.

Two bird nestlings exhibit different dietary compositions, MeHg sources, and levels. Nevertheless, their feathers exhibit comparable total Hg isotopic signatures (Figure 3C−F). This is because of the overlap of Hg isotopic compositions between emergent aquatic invertebrates and forest floor invertebrates. This is supported by the Hg isotopic mass balance during Hg transfer from invertebrates to nestlings (Figure S5). The forest floor invertebrates (>84%) are the primary contributor to the δ^{202}Hg and Δ^{199}Hg values in Niltava, and the signal from emergent aquatic invertebrates (>85%) dominates the δ^{202}Hg and Δ^{199}Hg values in Flycatcher. Both emergent aquatic and forest floor invertebrates shared similar Hg isotopic signals of decomposed forest litter or litter-submerged invertebrates (Figure 3A,B).

The predicted Hg isotopic values (except the Δ^{200}Hg) were calculated by Hg isotopic mass balance (Section S4), which did not completely match the measured values in birds (Figure

https://doi.org/10.1021/acs.est.3c10972
Environ. Sci. Technol. 2024, 58, 6007−6018

3C−F). The predicted δ^{202}Hg value is comparable to the measured δ^{202}Hg for Niltava (Figure 3E) but has a lower predicted value for Flycatcher (Figure 3C). The predicted Δ^{199}Hg values for both species are lower than the measured values. We attributed the discrepancy to several causes. One is that the remaining ∼30% (percentage of total food trips) of unknown food items might cause uncertainties in predicting Hg isotopes of nestling feathers. Additionally, MeHg and IHg may have individual Hg isotopic compositions,[83,84] but the model applies THg isotopic compositions for predicting the Hg isotopes in feathers. Finally, the maternal transfer is an additional cause[51,85] since adult birds have a larger foraging range, obtain different Hg isotopic signatures before breeding,[51] and then transfer these signals through egg-laying.[86]

We suggest that the last two causes seem more important. We compared the difference in %MeHg (i.e., the ratio of MeHg over THg) across trophic levels and observed the significant correlations between %MeHg and δ^{202}Hg (or Δ^{199}Hg). These correlations indicate that MeHg and IHg may have individual Hg isotopic compositions. However, % MeHg only explained less than 20% variations of δ^{202}Hg and Δ^{199}Hg across trophic levels (Figure S6). This suggests other Hg transfer pathways (e.g., maternal transfer), which, with different Hg isotopic signatures or fractionations, exist across the trophic levels.

4.4. Quantifying Hg Sources in Forest Bird Food Chains. Figure 4 shows that atmospheric Hg^0 is the main Hg source for most organisms in the food chains (15 out of 18 of the total measured species/category organisms, with >68% contribution from atmospheric Hg^0), except for 3 categories of canopy invertebrates (∼50% were from atmospheric Hg^{2+}). The higher contribution of atmospheric Hg^{2+} for the canopy invertebrates can be explained by invertebrates' direct or indirect uptake of cloudwater and fog containing high MeHg concentration[87,88] and positive Δ^{199}Hg and Δ^{200}Hg signals.[81] Our earlier work at Mt. Ailao has suggested that the moss and lichen on the canopy samples show Δ^{199}Hg and Δ^{200}Hg contributions from atmospheric Hg^{2+}.[89] Canopy invertebrates fed on these canopy biomasses can inherit the contribution of the atmospheric Hg^{2+} input. These observations indicate that MeHg in precipitation and fog may shape the MeHg biomagnifications in some canopy invertebrates and then transferred into the canopy birds.

5. IMPLICATIONS

Previous studies have established that bird MeHg levels were linked to their diets (with MeHg levels in the order of carnivores/piscivores > insectivores > omnivores > herbivores) and trophic position.[11,14,23] This study shows that forest insectivorous songbirds that forage on the forest floor (i.e., the understory insectivorous songbirds) are more vulnerable to MeHg exposure than songbirds that typically forage in the canopy. Montane forests are often characterized by humid conditions, high atmospheric Hg deposition loading through foliage uptake, and therefore favorable for the methylation on the forest floor.[3,40,41] Our study highlights that deposited atmospheric Hg is methylated into MeHg and then biomagnified in birds fed on the forest floor. We recommend further assessments on MeHg exposure for understory insectivorous birds and its ecological implication. This enables the understanding of how the change of atmospheric Hg loading can influence the risk of remote wildlife subject to global Hg pollution.

Given mainly MeHg elevated biomagnification in food webs,[19,22,61] the total Hg isotopes may not effectively elucidate Hg transfer in food chains.[83,84] The discrepancy between the predicted and measured Hg isotopic values of birds in this study confirms this hypothesis. We recommend further studies to use the speciation Hg isotopes, specifically MeHg isotopes, to trace the Hg transfer in forest bird food chains.

■ ASSOCIATED CONTENT

Supporting Information

The Supporting Information is available free of charge at https://pubs.acs.org/doi/10.1021/acs.est.3c10972.

Detailing bird breeding ecology surveys, sample collection, processing, and analyses; and nine tables summarizing the results and six figures illustrate the relationship between δ^{13}C and δ^{15}N, as well as the species/category positions in Figure 2 and the predicted contributions of Hg isotopes from invertebrates to birds (PDF)

■ AUTHOR INFORMATION

Corresponding Authors

Xun Wang − *State Key Laboratory of Environmental Geochemistry, Institute of Geochemistry, Chinese Academy of Sciences, Guiyang 550081, China;* orcid.org/0000-0002-7407-8965; Email: wangxun@ mail.gyig.ac.cn

Xinbin Feng − *State Key Laboratory of Environmental Geochemistry, Institute of Geochemistry, Chinese Academy of Sciences, Guiyang 550081, China; University of Chinese Academy of Sciences, Beijing 100049, China;* orcid.org/0000-0002-7462-8998; Email: fengxinbin@vip.skleg.cn

Authors

Kang Luo − *State Key Laboratory of Environmental Geochemistry, Institute of Geochemistry, Chinese Academy of Sciences, Guiyang 550081, China*

Wei Yuan − *State Key Laboratory of Environmental Geochemistry, Institute of Geochemistry, Chinese Academy of Sciences, Guiyang 550081, China*

Zhiyun Lu − *Ailaoshan Station for Subtropical Forest Ecosystem Studies, Chinese Academy of Sciences, Jingdong, Yunnan 676200, China*

Zichun Xiong − *Ailaoshan Station for Subtropical Forest Ecosystem Studies, Chinese Academy of Sciences, Jingdong, Yunnan 676200, China*

Che-Jen Lin − *Center for Advances in Water and Air Quality, Lamar University, Beaumont, Texas 77710, United States*

Complete contact information is available at: https://pubs.acs.org/10.1021/acs.est.3c10972

Notes

The authors declare no competing financial interest.

■ ACKNOWLEDGMENTS

This work was funded by the National Natural Science Foundation of China (42207311, 42122053). The authors are grateful for the assistance and permission of the Jingdong Bureau of Ailaoshan National Nature Reserve. The authors thank the staff from Ailaoshan Station for Subtropical Forest Ecosystem Research Studies (Qi Luo, Wenzheng Yang, Dawen

Li, Chengchang Luo, and Bicheng Yang) for their help in field bird-nest searching and checking. The data used in this study are tabulated in the Supporting Information.

REFERENCES

(1) Fitzgerald, W. F.; Engstrom, D. R.; Mason, R. P.; Nater, E. A. The Case for Atmospheric Mercury Contamination in Remote Areas. *Environ. Sci. Technol.* **1998**, *32* (1), 1−7.
(2) Lindberg, S.; Bullock, R.; Ebinghaus, R.; Engstrom, D.; Feng, X.; Fitzgerald, W.; Pirrone, N.; Prestbo, E.; Seigneur, C.; Panel on Source Attribution of Atmospheric Mercury. A synthesis of progress and uncertainties in attributing the sources of mercury in deposition. *Ambio* **2007**, *36* (1), 19−32, DOI: 10.1579/0044-7447(2007)36[19:asopau]2.0.co;2.
(3) Wang, X.; Luo, J.; Yin, R.; Yuan, W.; Lin, C. J.; Sommar, J.; Feng, X.; Wang, H.; Lin, C. Using Mercury Isotopes To Understand Mercury Accumulation in the Montane Forest Floor of the Eastern Tibetan Plateau. *Environ. Sci. Technol.* **2017**, *51* (2), 801−809.
(4) Wang, X.; Luo, J.; Yuan, W.; Lin, C. J.; Wang, F.; Liu, C.; Wang, G.; Feng, X. Global warming accelerates uptake of atmospheric mercury in regions experiencing glacier retreat. *Proc. Natl. Acad. Sci. U.S.A.* **2020**, *117* (4), 2049−2055.
(5) Lindqvist, O.; Johansson, K.; Bringmark, L.; Timm, B.; Aastrup, M.; Andersson, A.; Hovsenius, G.; Hkanson, L.; Iverfeldt, A.; Meili, M. Mercury in the Swedish environment? Recent research on causes, consequences and corrective methods. *Water, Air, Soil Pollut.* **1991**, *55* (1−2), xi−261.
(6) Morel, F. M. M.; Kraepiel, A. M. L.; Amyot, M. The Chemical Cycle and Bioaccumulation of Mercury. *Annu. Rev. Ecol. Syst.* **1998**, *29* (1), 543−566.
(7) Scheuhammer, A. M.; Meyer, M. W.; Sandheinrich, M. B.; Murray, M. W. Effects of environmental methylmercury on the health of wild birds, mammals, and fish. *Ambio* **2007**, *36* (1), 12−18.
(8) Scheuhammer, A.; Braune, B.; Chan, H. M.; Frouin, H.; Krey, A.; Letcher, R.; Loseto, L.; Noel, M.; Ostertag, S.; Ross, P.; Wayland, M. Recent progress on our understanding of the biological effects of mercury in fish and wildlife in the Canadian Arctic. *Sci. Total Environ.* **2015**, *509*−*510*, 91−103.
(9) UN-Environment. *Global Mercury Assessment 2018*; UN-Environment Programme, Chemicals and Health Branch: Geneva, Switzerland, 2019.
(10) Driscoll, C. T.; Mason, R. P.; Chan, H. M.; Jacob, D. J.; Pirrone, N. Mercury as a global pollutant: sources, pathways, and effects. *Environ. Sci. Technol.* **2013**, *47* (10), 4967−4983.
(11) Ackerman, J. T.; Eagles-Smith, C. A.; Herzog, M. P.; Hartman, C. A.; Peterson, S. H.; Evers, D. C.; Jackson, A. K.; Elliott, J. E.; Vander Pol, S. S.; Bryan, C. E. Avian mercury exposure and toxicological risk across western North America: A synthesis. *Sci. Total Environ.* **2016**, *568*, 749−769.
(12) Whitney, M. C.; Cristol, D. A. Impacts of sublethal mercury exposure on birds: A detailed review. *Rev. Environ. Contam. Toxicol.* **2017**, *244*, 113−163.
(13) Carravieri, A.; Vincze, O.; Bustamante, P.; Ackerman, J. T.; Adams, E. M.; Angelier, F.; Chastel, O.; Cherel, Y.; Gilg, O.; Golubova, E.; Kitaysky, A.; Luff, K.; Seewagen, C. L.; Strom, H.; Will, A. P.; Yannic, G.; Giraudeau, M.; Fort, J. Quantitative meta-analysis reveals no association between mercury contamination and body condition in birds. *Biol. Rev.* **2022**, *97*, 1253 DOI: 10.1111/brv.12840.
(14) Evers, D. C.; Burgess, N. M.; Champoux, L.; Hoskins, B.; Major, A.; Goodale, W. M.; Taylor, R. J.; Poppenga, R.; Daigle, T. Patterns and interpretation of mercury exposure in freshwater avian communities in northeastern north America. *Ecotoxicology* **2005**, *14* (1−2), 193−221.
(15) Rimmer, C. C.; McFarland, K. P.; Evers, D. C.; Miller, E. K.; Aubry, Y.; Busby, D.; Taylor, R. J. Mercury concentrations in Bicknell's thrush and other insectivorous passerines in Montane forests of northeastern North America. *Ecotoxicology* **2005**, *14* (1−2), 223−240.
(16) Rimmer, C. C.; Miller, E. K.; McFarland, K. P.; Taylor, R. J.; Faccio, S. D. Mercury bioaccumulation and trophic transfer in the terrestrial food web of a montane forest. *Ecotoxicology* **2010**, *19* (4), 697−709.
(17) Townsend, J. M.; Driscoll, C. T.; Rimmer, C. C.; McFarland, K. P. Avian, salamander, and forest floor mercury concentrations increase with elevation in a terrestrial ecosystem. *Environ. Toxicol. Chem.* **2014**, *33* (1), 208−215.
(18) Rodenhouse, N. L.; Lowe, W. H.; Gebauer, R. L. E.; McFarland, K. P.; Bank, M. S. Mercury bioaccumulation in temperate forest food webs associated with headwater streams. *Sci. Total Environ.* **2019**, *665*, 1125−1134.
(19) Li, C.; Xu, Z.; Luo, K.; Chen, Z.; Xu, X.; Xu, C.; Qiu, G. Biomagnification and trophic transfer of total mercury and methylmercury in a sub-tropical montane forest food web, southwest China. *Chemosphere* **2021**, *277*, No. 130371.
(20) Xiao, H.; Hu, Y.; Lang, Z.; Fang, B.; Guo, W.; Zhang, Q.; Pan, X.; Lu, X. How much do we know about the breeding biology of bird species in the world? *J. Avian Biol.* **2017**, *48* (4), 513−518.
(21) Townsend, J. M.; Rimmer, C. C.; Driscoll, C. T.; McFarland, K. P.; Inigo-Elias, E. Mercury concentrations in tropical resident and migrant songbirds on Hispaniola. *Ecotoxicology* **2013**, *22* (1), 86−93.
(22) Luo, K.; Xu, Z.; Wang, X.; Quan, R.-C.; Lu, Z.; Bi, W.; Zhao, H.; Qiu, G. Terrestrial methylmercury bioaccumulation in a pine forest food chain revealed by live nest videography observations and nitrogen isotopes. *Environ. Pollut.* **2020**, *263*, No. 114530, DOI: 10.1016/j.envpol.2020.114530.
(23) Ackerman, J. T.; Hartman, C. A.; Herzog, M. P. Mercury contamination in resident and migrant songbirds and potential effects on body condition. *Environ. Pollut.* **2019**, *246*, 797−810.
(24) Abeysinghe, K. S.; Qiu, G.; Goodale, E.; Anderson, C. W. N.; Bishop, K.; Evers, D. C.; Goodale, M. W.; Hintelmann, H.; Liu, S.; Mammides, C.; Quan, R. C.; Wang, J.; Wu, P.; Xu, X. H.; Yang, X. D.; Feng, X. Mercury flow through an Asian rice-based food web. *Environ. Pollut.* **2017**, *229*, 219−228.
(25) Lavoie, R. A.; Hebert, C. E.; Rail, J. F.; Braune, B. M.; Yumvihoze, E.; Hill, L. G.; Lean, D. R. Trophic structure and mercury distribution in a Gulf of St. Lawrence (Canada) food web using stable isotope analysis. *Sci. Total Environ.* **2010**, *408* (22), 5529−5539.
(26) Hoenig, B. D.; Snider, A. M.; Forsman, A. M.; Hobson, K. A.; Latta, S. C.; Miller, E. T.; Polito, M. J.; Powell, L. L.; Rogers, S. L.; Sherry, T. W.; Toews, D. P. L.; Welch, A. J.; Taylor, S. S.; Porter, B. A. Current methods and future directions in avian diet analysis. *Ornithology* **2022**, *139* (1), No. ukab077, DOI: 10.1093/ornithology/ukab077.
(27) Tsui, M. T. K.; Blum, J. D.; Kwon, S. Y.; Finlay, J. C.; Balogh, S. J.; Nollet, Y. H. Sources and transfers of methylmercury in adjacent river and forest food webs. *Environ. Sci. Technol.* **2012**, *46* (20), 10957−10964.
(28) Tsui, M.-K.; Blum, J. D.; Kwon, S. Y. Review of stable mercury isotopes in ecology and biogeochemistry. *Sci. Total Environ.* **2020**, *716*, No. 135386.
(29) Li, M. L.; Kwon, S. Y.; Poulin, B. A.; Tsui, M. T.; Motta, L. C.; Cho, M. Internal Dynamics and Metabolism of Mercury in Biota: A Review of Insights from Mercury Stable Isotopes. *Environ. Sci. Technol.* **2022**, *56* (13), 9182−9195.
(30) Luo, K.; Feng, L.; Lu, Z.; Li, D.; Quan, R.-C. Novel instance of brood parasitic cuckoo nestlings using bright yellow patches to mimic gapes of host nestlings. *Wilson J. Ornithol.* **2019**, *131* (3), 686−693, DOI: 10.1676/18-168.
(31) Sinkovics, C.; Seress, G.; Fábián, V.; Sándor, K.; Liker, A. Obtaining accurate measurements of the size and volume of insects fed to nestlings from video recordings. *J. Field Ornithol.* **2018**, *89* (2), 165−172.
(32) Blum, J. D.; Sherman, L. S.; Johnson, M. W. Mercury Isotopes in Earth and Environmental Sciences. *Annu. Rev. Earth Planet. Sci.* **2014**, *42* (1), 249−269.
(33) Yin, R.; Krabbenhoft, D. P.; Bergquist, B. A.; Zheng, W.; Lepak, R. F.; Hurley, J. P. Effects of mercury and thallium concentrations on

https://doi.org/10.1021/acs.est.3c10972
Environ. Sci. Technol. 2024, 58, 6007−6018

high precision determination of mercury isotopic composition by Neptune Plus multiple collector inductively coupled plasma mass spectrometry. *J. Anal. At. Spectrom.* **2016**, *31* (10), 2060−2068.
(34) Kwon, S. Y.; Blum, J. D.; Carvan, M. J.; Basu, N.; Head, J. A.; Madenjian, C. P.; David, S. R. Absence of fractionation of mercury isotopes during trophic transfer of methylmercury to freshwater fish in captivity. *Environ. Sci. Technol.* **2012**, *46* (14), 7527−7534.
(35) Kwon, S. Y.; Blum, J. D.; Chen, C. Y.; Meattey, D. E.; Mason, R. P. Mercury isotope study of sources and exposure pathways of methylmercury in estuarine food webs in the Northeastern U.S. *Environ. Sci. Technol.* **2014**, *48* (17), 10089−10097.
(36) Zhang, L.; Yin, Y.; Li, Y.; Cai, Y. Mercury isotope fractionation during methylmercury transport and transformation: A review focusing on analytical method, fractionation characteristics, and its application. *Sci. Total Environ.* **2022**, *841*, No. 156558.
(37) Liu, H. W.; Yu, B.; Yang, L.; Wang, L. L.; Fu, J. J.; Liang, Y.; Bu, D.; Yin, Y. G.; Hu, L. G.; Shi, J. B.; Jiang, G. B. Terrestrial mercury transformation in the Tibetan Plateau: New evidence from stable isotopes in upland buzzards. *J. Hazard. Mater.* **2020**, *400*, No. 123211.
(38) Zheng, W.; Zhao, Y. Q.; Sun, R. Y.; Chen, J. B. The Mechanism of Mercury Stable Isotope Fractionation: A Review. *Bull. Mineral., Petrol. Geochem.* **2021**, *40*, 1087−1110.
(39) Xu, Z.; Lu, Q.; Xu, X.; Liang, L.; Abeysinghe, K. S.; Chen, Z.; Qiu, G. Aquatic methylmercury is a significant subsidy for terrestrial songbirds: Evidence from the odd mass-independent fractionation of mercury isotopes. *Sci. Total Environ.* **2023**, *880*, No. 163217.
(40) Blackwell, B. D.; Driscoll, C. T. Deposition of Mercury in Forests along a Montane Elevation Gradient. *Environ. Sci. Technol.* **2015**, *49* (9), 5363−5370.
(41) Zhang, H.; Yin, R. S.; Feng, X. B.; Sommar, J.; Anderson, C. W.; Sapkota, A.; Fu, X. W.; Larssen, T. Atmospheric mercury inputs in montane soils increase with elevation: evidence from mercury isotope signatures. *Sci. Rep.* **2013**, *3*, No. 3322, DOI: 10.1038/srep03322.
(42) Yuan, W.; Sommar, J.; Lin, C.-J.; Wang, X.; Li, K.; Liu, Y.; Zhang, H.; Lu, Z.; Wu, C.; Feng, X. Stable Isotope Evidence Shows Re-emission of Elemental Mercury Vapor Occurring after Reductive Loss from Foliage. *Environ. Sci. Technol.* **2019**, *53* (2), 651−660.
(43) Yuan, W.; Wang, X.; Lin, C. J.; Wu, C.; Zhang, L.; Wang, B.; Sommar, J.; Lu, Z.; Feng, X. Stable Mercury Isotope Transition during Postdepositional Decomposition of Biomass in a Forest Ecosystem over Five Centuries. *Environ. Sci. Technol.* **2020**, *54* (14), 8739−8749.
(44) Yuan, W.; Wang, X.; Lin, C. J.; Wu, F.; Luo, K.; Zhang, H.; Lu, Z.; Feng, X. Mercury Uptake, Accumulation, and Translocation in Roots of Subtropical Forest: Implications of Global Mercury Budget. *Environ. Sci. Technol.* **2022**, *56* (19), 14154−14165.
(45) Han-Dong, W.; Lin, L.; Yang, J.; Hu, Y.; Cao, M.; Liu, Y.; Lu, Z.; Xie, Y. Species composition and community structure of a 20 hm2 plot of mid-mountain moist evergreen broad-leaved forest on the Mts. Ailaoshan, Yunnan Province, China. *Chin. J. Plant Ecol.* **2018**, *42* (4), 419−429.
(46) BirdLife-International. Important Bird Area Factsheet: Ailaoshan, 2023. Downloaded from http://datazone.birdlife.org/site/factsheet/ailaoshan-iba-china-(mainland) on Aug 05, 2023.
(47) Wang, X.; Yuan, W.; Lin, C. J.; Zhang, L.; Zhang, H.; Feng, X. Climate and Vegetation As Primary Drivers for Global Mercury Storage in Surface Soil. *Environ. Sci. Technol.* **2019**, *53* (18), 10665−10675.
(48) Wang, X.; Yuan, W.; Lin, C. J.; Wu, F.; Feng, X. Stable mercury isotopes stored in Masson Pinus tree rings as atmospheric mercury archives. *J. Hazard. Mater.* **2021**, *415*, No. 125678.
(49) Wang, X.; Yuan, W.; Feng, X.; Wang, D.; Luo, J. Moss facilitating mercury, lead and cadmium enhanced accumulation in organic soils over glacial erratic at Mt. Gongga, China. *Environ. Pollut.* **2019**, *254* (Pt A), No. 112974.
(50) Wang, X.; Yuan, W.; Lin, C. J.; Luo, J.; Wang, F.; Feng, X.; Fu, X.; Liu, C. Underestimated Sink of Atmospheric Mercury in a Deglaciated Forest Chronosequence. *Environ. Sci. Technol.* **2020**, *54* (13), 8083−8093.
(51) Xu, Z.; Luo, K.; Lu, Q.; Shang, L.; Tian, J.; Lu, Z.; Li, Q.; Chen, Z.; Qiu, G. The mercury flow through a terrestrial songbird food chain in subtropical pine forest: Elucidated by Bayesian isotope mixing model and stable mercury isotopes. *J. Hazard. Mater.* **2023**, *459*, No. 132263.
(52) Zhang, F.; Xu, Z.; Xu, X.; Liang, L.; Chen, Z.; Dong, X.; Luo, K.; Dinis, F.; Qiu, G. Terrestrial mercury and methylmercury bioaccumulation and trophic transfer in subtropical urban forest food webs. *Chemosphere* **2022**, *299*, No. 134424.
(53) Hammerschmidt, C. R.; Fitzgerald, W. F. Methylmercury in mosquitoes related to atmospheric mercury deposition and contamination. *Environ. Sci. Technol.* **2005**, *39* (9), 3034−3039.
(54) Tsz-Ki Tsui, M.; Liu, S.; Brasso, R. L.; Blum, J. D.; Kwon, S. Y.; Ulus, Y.; Nollet, Y. H.; Balogh, S. J.; Eggert, S. L.; Finlay, J. C. Controls of Methylmercury Bioaccumulation in Forest Floor Food Webs. *Environ. Sci. Technol.* **2019**, *53* (5), 2434−2440.
(55) Qin, C.; Du, B.; Yin, R.; Meng, B.; Fu, X.; Li, P.; Zhang, L.; Feng, X. Isotopic Fractionation and Source Appointment of Methylmercury and Inorganic Mercury in a Paddy Ecosystem. *Environ. Sci. Technol.* **2020**, *54* (22), 14334−14342.
(56) Yin, R.-S.; Feng, X.-B.; Foucher, D.; Shi, W.-F.; Zhao, Z.-Q.; Wang, J. High Precision Determination of Mercury Isotope Ratios Using Online Mercury Vapor Generation System Coupled with Multicollector Inductively Coupled Plasma-Mass Spectrometer. *Chin. J. Anal. Chem.* **2010**, *38* (7), 929−934.
(57) Bergquist, B. A.; Blum, J. D. Mass-Dependent and -Independent Fractionation of Hg Isotopes by Photoreduction in Aquatic Systems. *Science* **2007**, *318* (5849), 417−420.
(58) Estrade, N.; Carignan, J.; Sonke, J. E.; Donard, O. F. X. Measuring Hg Isotopes in Bio-Geo-Environmental Reference Materials. *Geostand. Geoanal. Res.* **2010**, *34* (1), 79−93.
(59) Blum, J. D.; Bergquist, B. A. Reporting of variations in the natural isotopic composition of mercury. *Anal. Bioanal. Chem.* **2007**, *388* (2), 353−359.
(60) Post, D. M. Using Stable Isotopes to Estimate Trophic Position: Models, Methods, and Assumptions. *Ecology* **2002**, *83* (3), 703−718.
(61) Lavoie, R. A.; Jardine, T. D.; Chumchal, M. M.; Kidd, K. A.; Campbell, L. M. Biomagnification of mercury in aquatic food webs: a worldwide meta-analysis. *Environ. Sci. Technol.* **2013**, *47* (23), 13385−13394.
(62) Rich, C. D.; Blaine, A. C.; Hundal, L.; Higgins, C. P. Bioaccumulation of perfluoroalkyl acids by earthworms (Eisenia fetida) exposed to contaminated soils. *Environ. Sci. Technol.* **2015**, *49* (2), 881−888.
(63) Yung, L.; Bertheau, C.; Cazaux, D.; Regier, N.; Slaveykova, V. I.; Chalot, M. Insect Life Traits Are Key Factors in Mercury Accumulation and Transfer within the Terrestrial Food Web. *Environ. Sci. Technol.* **2019**, *53* (19), 11122−11132.
(64) Yu, L. H.; Luo, X. J.; Wu, J. P.; Liu, L. Y.; Song, J.; Sun, Q. H.; Zhang, X. L.; Chen, D.; Mai, B. X. Biomagnification of higher brominated PBDE congeners in an urban terrestrial food web in north China based on field observation of prey deliveries. *Environ. Sci. Technol.* **2011**, *45* (12), 5125−5131.
(65) Vainio, R. K.; Jormalainen, V.; Dietz, R.; Laaksonen, T.; Schulz, R.; Sonne, C.; Sondergaard, J.; Zubrod, J. P.; Eulaers, I. Trophic Dynamics of Mercury in the Baltic Archipelago Sea Food Web: The Impact of Ecological and Ecophysiological Traits. *Environ. Sci. Technol.* **2022**, *56* (16), 11440−11448.
(66) Jiskra, M.; Wiederhold, J. G.; Skyllberg, U.; Kronberg, R. M.; Hajdas, I.; Kretzschmar, R. Mercury deposition and re-emission pathways in boreal forest soils investigated with Hg isotope signatures. *Environ. Sci. Technol.* **2015**, *49* (12), 7188−7196.
(67) Obrist, D.; Pearson, C.; Webster, J.; Kane, T.; Lin, C. J.; Aiken, G. R.; Alpers, C. N. A synthesis of terrestrial mercury in the western United States: Spatial distribution defined by land cover and plant productivity. *Sci. Total Environ.* **2016**, *568*, 522−535.

(68) Feng, X.; Wang, X.; Sun, G.; Yuan, W. Research Progresses and Challenges of Mercury Biogeochemical Cycling in Global Vegetation Ecosystem. *J. China Univ. Geosci.* **2022**, *47* (11), 4098.
(69) Wang, X.; Yuan, W.; Lin, C.-J.; Feng, X. Mercury cycling and isotopic fractionation in global forests. *Crit. Rev. Environ. Sci. Technol.* **2022**, *52* (21), 3763−3786.
(70) Sun, R.; Jiskra, M.; Amos, H. M.; Zhang, Y.; Sunderland, E. M.; Sonke, J. E. Modelling the mercury stable isotope distribution of Earth surface reservoirs: Implications for global Hg cycling. *Geochim. Cosmochim. Acta* **2019**, *246*, 156−173.
(71) Li, K.; Lin, C.-J.; Yuan, W.; Sun, G.; Fu, X.; Feng, X. An improved method for recovering and preconcentrating mercury in natural water samples for stable isotope analysis. *J. Anal. At. Spectrom.* **2019**, *34* (11), 2303−2313.
(72) Wang, X.; Lin, C. J.; Lu, Z. Y.; Zhang, H.; Zhang, Y. P.; Feng, X. B. Enhanced accumulation and storage of mercury on subtropical evergreen forest floor: Implications on mercury budget in global forest ecosystems. *J. Geophys. Res.: Biogeosci.* **2016**, *121* (8), 2096−2109.
(73) Lu, Z.; Yuan, W.; Luo, K.; Wang, X. Litterfall mercury reduction on a subtropical evergreen broadleaf forest floor revealed by multi-element isotopes. *Environ. Pollut.* **2021**, *268* (Pt A), No. 115867.
(74) Jardine, T. D.; Kidd, K. A.; O'Driscoll, N. Food web analysis reveals effects of pH on mercury bioaccumulation at multiple trophic levels in streams. *Aquat. Toxicol.* **2013**, *132*−*133*, 46−52.
(75) Steffan, S. A.; Chikaraishi, Y.; Dharampal, P. S.; Pauli, J. N.; Guedot, C.; Ohkouchi, N. Unpacking brown food-webs: Animal trophic identity reflects rampant microbivory. *Ecol. Evol.* **2017**, *7* (10), 3532−3541.
(76) Wang, B.; Yuan, W.; Wang, X.; Li, K.; Lin, C. J.; Li, P.; Lu, Z.; Feng, X.; Sommar, J. Canopy-Level Flux and Vertical Gradients of Hg(0) Stable Isotopes in Remote Evergreen Broadleaf Forest Show Year-Around Net Hg(0) Deposition. *Environ. Sci. Technol.* **2022**, *56* (9), 5950−5959.
(77) Twining, C. W.; Razavi, N. R.; Brenna, J. T.; Dzielski, S. A.; Gonzalez, S. T.; Lawrence, P.; Cleckner, L. B.; Flecker, A. S. Emergent Freshwater Insects Serve as Subsidies of Methylmercury and Beneficial Fatty Acids for Riparian Predators Across an Agricultural Gradient. *Environ. Sci. Technol.* **2021**, *55* (9), 5868−5877.
(78) Cristol, D. A.; Brasso, R. L.; Condon, A. M.; Fovargue, R. E.; Friedman, S. L.; Hallinger, K. K.; Monroe, A. P.; White, A. E. The movement of aquatic mercury through terrestrial food webs. *Science* **2008**, *320* (5874), 335 DOI: 10.1126/science.1154082.
(79) Woerndle, G. E.; Tsz-Ki Tsui, M.; Sebestyen, S. D.; Blum, J. D.; Nie, X.; Kolka, R. K. New Insights on Ecosystem Mercury Cycling Revealed by Stable Isotopes of Mercury in Water Flowing from a Headwater Peatland Catchment. *Environ. Sci. Technol.* **2018**, *52* (4), 1854−1861.
(80) Jiskra, M.; Wiederhold, J. G.; Skyllberg, U.; Kronberg, R. M.; Kretzschmar, R. Source tracing of natural organic matter bound mercury in boreal forest runoff with mercury stable isotopes. *Environ. Sci.: Processes Impacts* **2017**, *19* (10), 1235−1248.
(81) Chen, J.; Hintelmann, H.; Zheng, W.; Feng, X.; Cai, H.; Wang, Z.; Yuan, S.; Wang, Z. Isotopic evidence for distinct sources of mercury in lake waters and sediments. *Chem. Geol.* **2016**, *426*, 33−44.
(82) Li, K. The Source and Sink of Mercury in Throughfall and Runoff of Four Typical Forest Catchments. Ph.D. Thesis, Institute of Geochemistry, Chinese Academy of Sciences, 2022.
(83) Yang, S.; Li, P.; Liu, J.; Ubaid Ali, M.; Ding, L.; Wang, B. Combining of C, N and specific Hg stable isotopes to track bioaccumulation of monomethylmercury in coastal and freshwater seafood. *Food Chem.* **2023**, *401*, No. 134202.
(84) Li, P.; Du, B.; Maurice, L.; Laffont, L.; Lagane, C.; Point, D.; Sonke, J. E.; Yin, R.; Lin, C. J.; Feng, X. Mercury Isotope Signatures of Methylmercury in Rice Samples from the Wanshan Mercury Mining Area, China: Environmental Implications. *Environ. Sci. Technol.* **2017**, *51* (21), 12321−12328.
(85) Ackerman, J. T.; Eagles-Smith, C. A.; Herzog, M. P. Bird mercury concentrations change rapidly as chicks age: toxicological risk is highest at hatching and fledging. *Environ. Sci. Technol.* **2011**, *45* (12), 5418−5425.
(86) Ackerman, J. T.; Herzog, M. P.; Schwarzbach, S. E. Methylmercury is the predominant form of mercury in bird eggs: a synthesis. *Environ. Sci. Technol.* **2013**, *47* (4), 2052−2060.
(87) St Louis, V. L.; Rudd, J. W.; Kelly, C. A.; Hall, B. D.; Rolfhus, K. R.; Scott, K. J.; Lindberg, S. E.; Dong, W. Importance of the forest canopy to fluxes of methyl mercury and total mercury to boreal ecosystems. *Environ. Sci. Technol.* **2001**, *35* (15), 3089−3098.
(88) Weiss-Penzias, P. S.; Ortiz, C.; Acosta, R. P.; Heim, W.; Ryan, J. P.; Fernandez, D.; Collett, J. L.; Flegal, A. R. Total and monomethyl mercury in fog water from the central California coast. *Geophys. Res. Lett.* **2012**, *39* (3), No. L03804, DOI: 10.1029/2011GL050324.
(89) Li, X.; Wang, X.; Zhang, H.; Lu, Z. Y. Mosses and lichens enhance atmospheric elemental mercury deposition in a subtropical montane forest. *Environ. Chem.* **2023**, *20* (3), 105−113.

https://doi.org/10.1021/acs.est.3c10972
Environ. Sci. Technol. 2024, 58, 6007−6018